Design of Rotman Type Lens for Multiple Beam forming

Ravi Pratap Singh Kushwah, P.K. Singhal & P.C. Sharma*

Department of Electronics
Madhav Institute of Technology & Science, Gwalior-474 005, India
E-mail: kushwah.ravipratapsingh@rediffmail.com & pks_65@yahoo.com
*S.D. Bansal College of Engineering, Indore, India

Abstract- **Design of Rotman type beam forming bootlace lens have been discussed. Scattering matrix of the bootlace lens has been evaluated using the contour integral approach. Radiation characteristics of the bootlace lens have been investigated with different types of the micorstrip antenna.**

Index terms- **Bootlace lens, Butler matrix, microstrip antenna, electronically scanning and contour integral approach.**

I. INTRODUCTION:

Rotman type bootlace lens [1, 2] is an useful tool for multiple beam forming, because of its frequency independent characteristics. It is more commonly preferred over Butler matrix [3]. Four design approaches [1, 4, 5, 6] have been so are reported for the design of Rotman type bootlace lens. Basically all the design approaches are based on phase shift comparison. Lot of research work have been reported [7-14] to improve the performance of the lens, in term of amplitude coupling between input and output ports and phase along the radiating elements.

In the present work Rotman type bootlace lens has been designed at 2.00 GHz. Two-dimensional field analysis of the designed bootlace lens has been carried out using the contour integral approach. Radiation characteristics of the lens have been investigated with different types of microstrip antennas.

Rotman type lens

Figure 1 shows the cross-section of Rotman lens. One feed point F_o is located on the axis of the lens and two other feed points F_1 and F_2 are located either side of the axis of the lens at focal angles $+\alpha$ and $-\alpha$ respectively on a circular focal arc. Array elements are located along the straight line I_2. The array elements are connected to the inner surface of the lens I_1 through TEM mode transmission line. The inner surface of the lens is called array contour. A general point P(X, Y) defines the array contour. Distance from point O_1 to F_o is called the on axis focal length. Distance from O_1 to F_1 or F_2 is called the off axis focal length.

The array contour and the transmission lines are designed in such a way that the outgoing beam makes an angle $-\alpha$, 0 and α with the axis of the lens and terminates perpendicular to the respective wave-front, when feed is placed at F_1, F_0 and F_2 respectively.

Figure 2 shows the direction of the outgoing beam for the three feed points. A ray originating from point F_1 on the feed contour may reach the wave-front from F_1 to O_1, transmission W (0), point Q_2 and terminates normal to the wave-front. Also the ray may reach the wave-front through a general point P(X, Y) on the array contour, transmission line W (N), point Q(N) and then tracing a straight line at an angle $-\alpha$. Similarly rays from F_1 and F_2 may reach their respective wave-front.

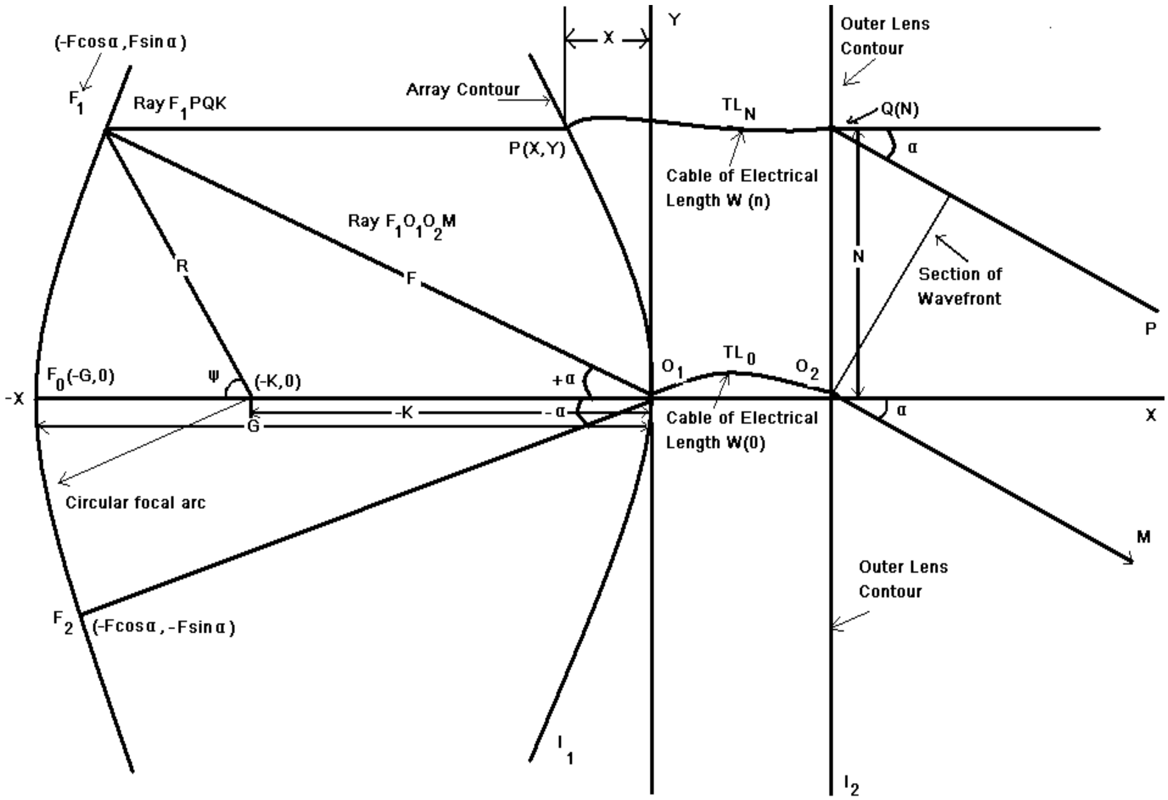

Fig. 1: Cross-section of Rotman Lens Geometry

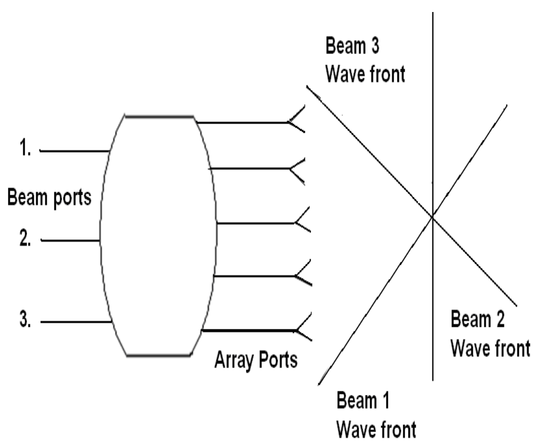

Fig. 2: Direction of the outgoing beam for input at different feed ports

The array contour and the transmission lines are designed from the design equations can be derived using the fact that at the wave-front all the rays must be in phase independent of the path they travel. This requires that the total phase shift in traversing the path to reach the wave-front in each case be equal. The design equations have been derived in [1, 2].

In the present work Rotman type lens was designed for the following requirements:

Scanning angle: + 35° to -35°
Number of array elements: 10
Number of input ports: 09
Frequency: 2.00 GHz

The complete structure is assumed to be fabricated on a substrate of thickness 1.60 mm and dielectric constant 4.4 and loss tangent 0.02.

To design the lens using the design equations given in [1, 2] the following design parameters were selected

Off axis focal length = 1.448 λ
On axis focal length = 1.718 λ
Antenna element spacing = 2.78 cm
α = 35°
Total array length = 25.19 cm

Considering the effect of off axis focal length and on axis focal length [7], the suitable values of the design parameters were selected to maximize the coupling from the input ports to output ports. Suitable values of antenna element spacing were also selected to avoid the grating lobes.

The designed lens is shown in figure 3. As per the given requirements, the feed contour has nine input ports and array contour has ten output ports.

The feed contour and array contour are the open boundaries. Two dummy ports were provided to cover the gap between the feed contour and the array contour on the upper side of the lens and two dummy ports were provided in lower side. Therefore the lens has total 23 ports. The dummy ports are terminated to 50 ohms dummy load to avoid the internal reflections. The input and the output ports are connected to source and antenna elements respectively through 50 ohms transmission lines. The 50 ohms transmission lines are connected to lens ports through taper sections to avoid the impedance mismatch. The lens with taper sections is shown in figure 4. Port number 2 to 11 are the antenna ports, port number 14 to 22 are the input ports. The port number 1, 12, 13 and 23 are the dummy ports. Same port number notation will be used in the following sections. Table 1 shows the width of output ports and dummy ports. The width of the output ports were optimized for uniform coupling (as much as possible) from each input ports. Width of each input port is equal and it is 0.7094091 inch.

Table 1: Width of output and dummy ports

Port No. (Output ports)	Port width in inch	Port No. (Dummy Ports)	Port width in inch
2	0.5457740	1	1.256912
3	0.5007070	12	1.256912
4	0.4855116	13	1.125953
5	0.4770660	23	1.125953
6	0.4732057		
7	0.4732057		
8	0.4770660		
9	0.4855116		
10	0.5007070		
11	0.5457740		

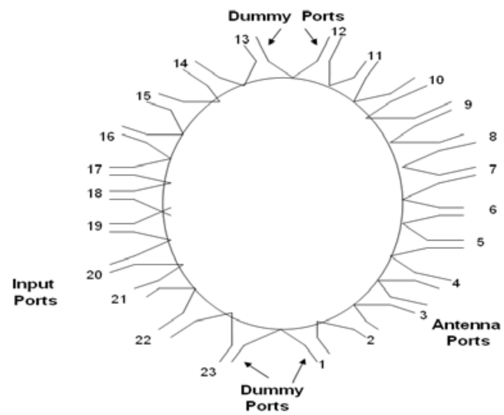

Fig. 3: Lens in its multiport geometry

Figure 4 shows the taper section, length of the taper section is 1.085λ. Length of the taper section is equal for all the ports.

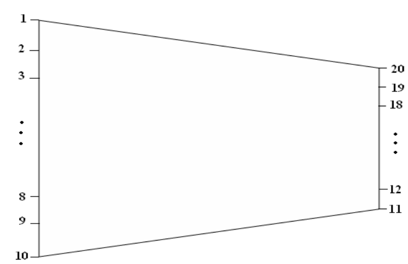

Fig. 4: Taper section

The length was selected in such a manner that the magnitude of the reflection coefficient for each port must be less than 0.01. The magnitude of the reflection coefficient was evaluated using the contour integral approach (discussed in the next section). Layout of the finally designed lens is shown in figure 5.

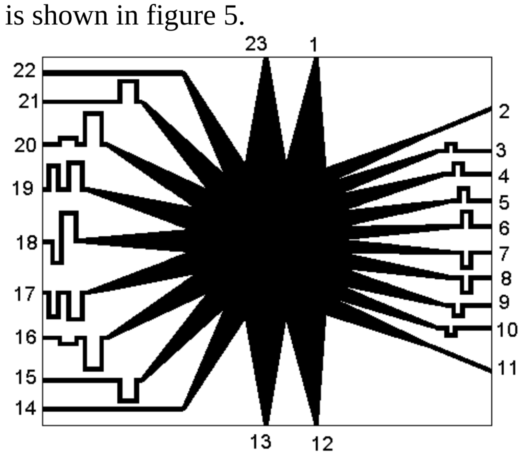

Fig. 5: Layout of the designed lens along with the port numbers

Two dimensional field analysis of the lens

In microstrip or strip line configuration, height of the lens is much smaller than the wave-length at the operating frequencies and consequently there is no variation of the field along the height of the substrate. This type of planar circuit may be considered as a two dimensional circuit. Because of the arbitrary geometrical shape of the lens, contour integral method has been adopted to analyze the designed lens. More details of the contour integral approach have been given in [15, 16].

To analyze the lens, Z-matrix of the lens without Z-matrices for the lens without taper and for the taper sections are calculated separately. For Z-matrix calculation of the lens without taper, each port of the lens is further divided into ten subports. So the Z-matrix of the lens without taper is 230X230 matrixes. For Z-matrix calculation of the taper, both ends of the taper have been divided in ten subports and the length of the taper has been divided in into 90 subports. Overall, the Z-matrix of the lens with the taper section is obtained by combining the Z-matrix of the lens without taper with Z-matrices of the taper sections using the segmentation approach [17]. The overall Z-matrix thus obtained is of the order of 230X230. The multiple subports at each external port are combined using the approach suggested in [17].

The S-matrix of the lens is computed from the Z-matrix with 50 ohms line termination at each end. Radiation patterns for the array elements are computed using the voltage distribution for the given spacing between the array elements. The array elements in the present case are microstrip antennas.

II. RESULTS AND DISCUSSION

Figure 6 shows the reflection coefficient at the input ports. In view of the geometrical symmetry of the lens results for only half of the input ports are shown.

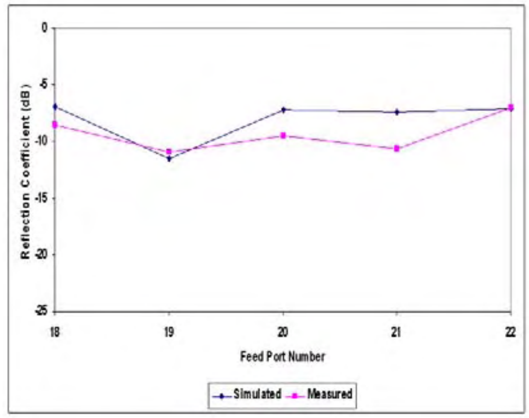

Fig. 6: Reflection coefficients at the input ports

Figure 7(a-e) shows the coupling from the input ports to output ports. Table 2 shows the coupling from the input ports to four dummy ports.

Table 2: Coupling from the input ports to dummy ports

Dummy Port No.	Input port Number									
	18		19		20		21		22	
	M	S	M	S	M	S	M	S	M	S
1	-17.7	-16.8	-20.1	-21.7	-19.9	-19.1	-19.0	-19.1	-22.0	-22.0
12	-19.0	-21.2	-16.5	-18.4	-16.6	-17.0	-16.5	-16.3	-11.0	-15.0
13	-17.8	-16.8	-16.1	-17.6	-10.7	-16.9	-16.9	-16.8	-11.3	-16.0
14	-21.7	-21.2	-16.4	-16.1	-13.3	-17.6	-20.0	-16.8	-10.0	-11.0

M – Measure Values; S – Simulated Values; All the values are in dB

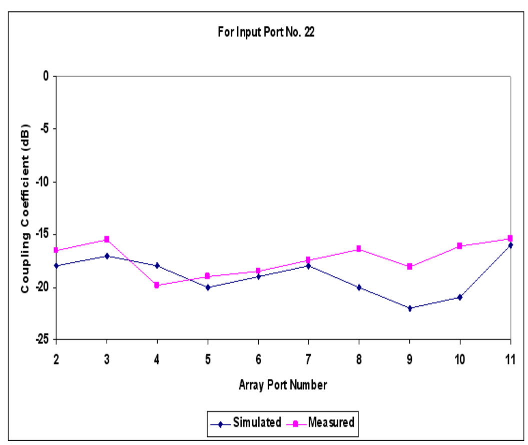

Fig. 7(a): Amplitude coupling from input port No. 22 to output ports

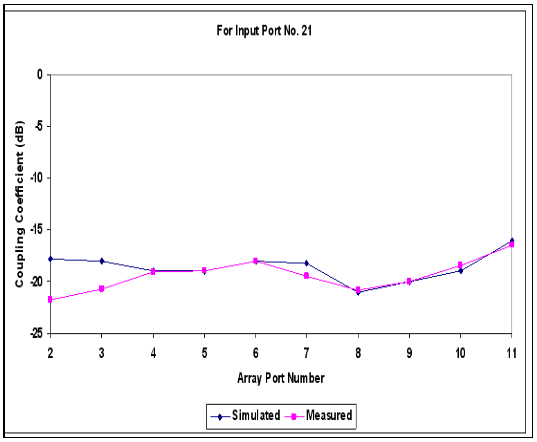

Fig. 7(b): Amplitude coupling from input port No. 21 to output ports

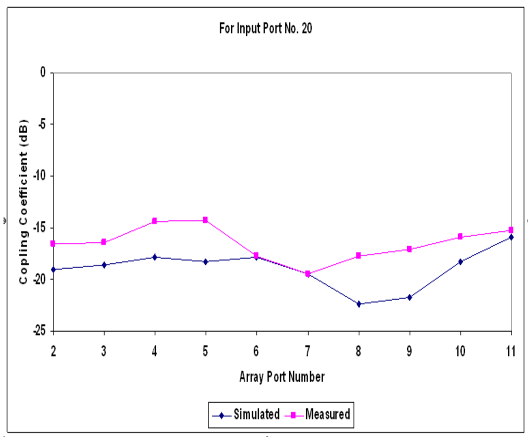

Fig. 7(c): Amplitude coupling from input port No. 20 to output ports

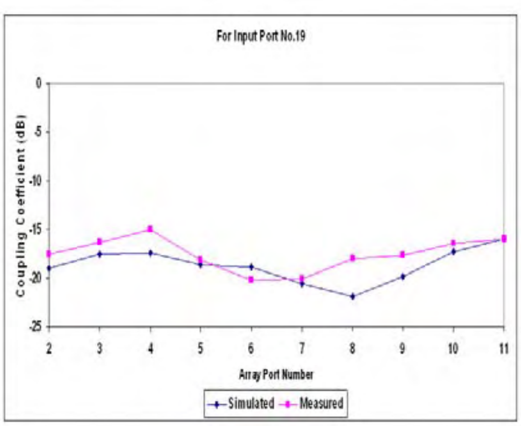

Fig. 7(d): Amplitude coupling from input port No. 19 to output ports

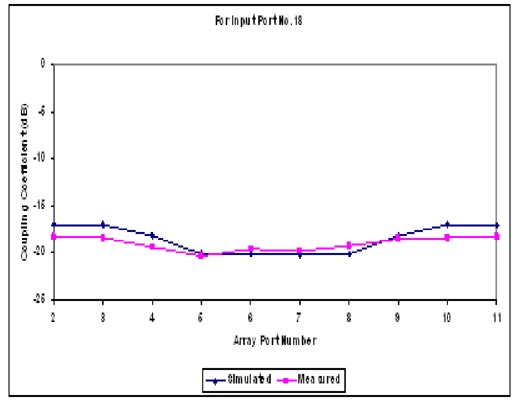

Fig. 7(e): Amplitude coupling from input port No. 18 to output ports

Radiation characteristics of the bootlace lens were determined using different types of radiating elements. A rectangular microstrip antenna was designed for operation at 2.00 GHz. The designed antenna is shown in figure 8.

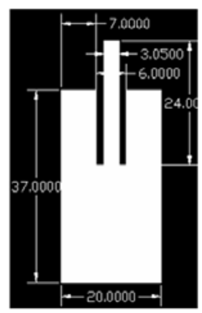

Fig. 8: Designed microstrip antenna (All the dimensions are in mm)

The designed microstrip antenna was simulated using commercially available software IE3D [18]. Figure 9, shows the variation of return loss with frequency, the designed antenna is operating at 2.00 GHz.

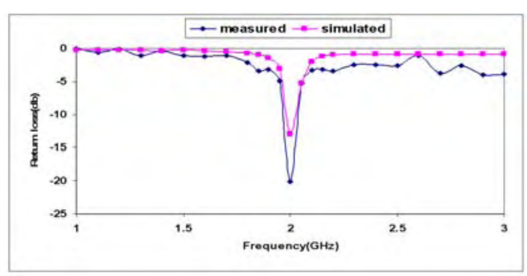

Fig 9: Variation of Return Loss with frequency for the designed microstrip antenna

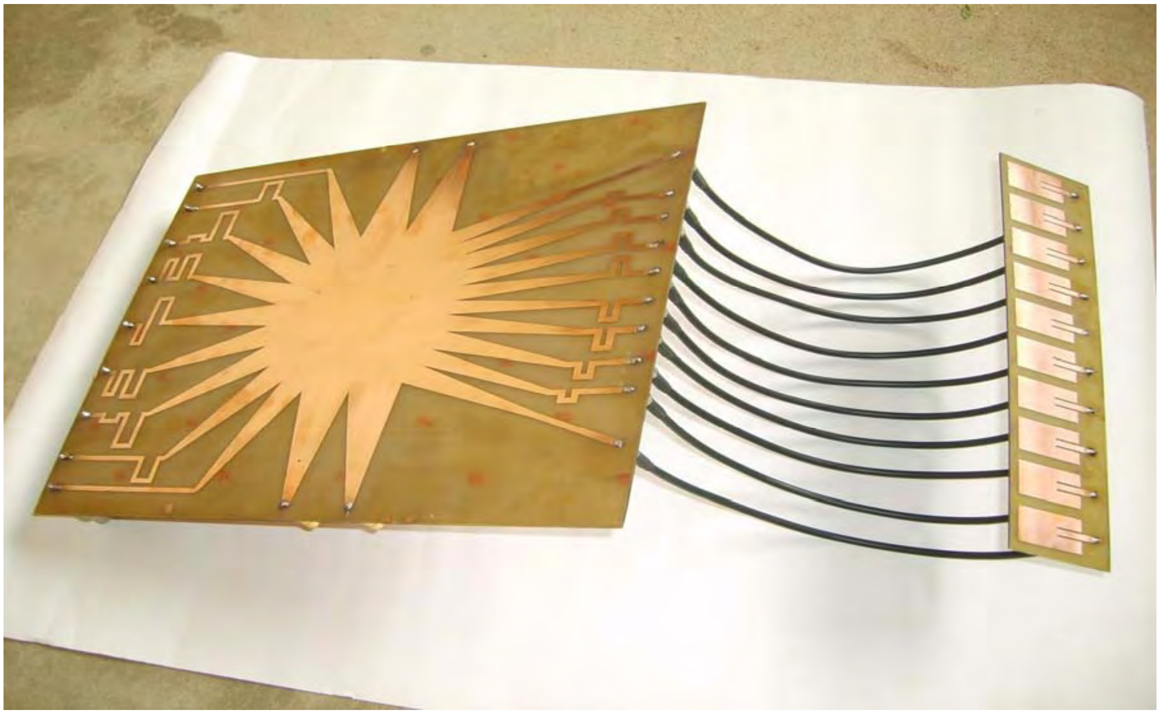

Fig. 10: Designed Rotman Lens

Figure 10 shows the photograph of the bootlace lens along with the microstrip antenna array.

Figure 11(a-e) shows the radiation pattern for input at different feed ports. For each input ports the direction of the outgoing beam is changing.

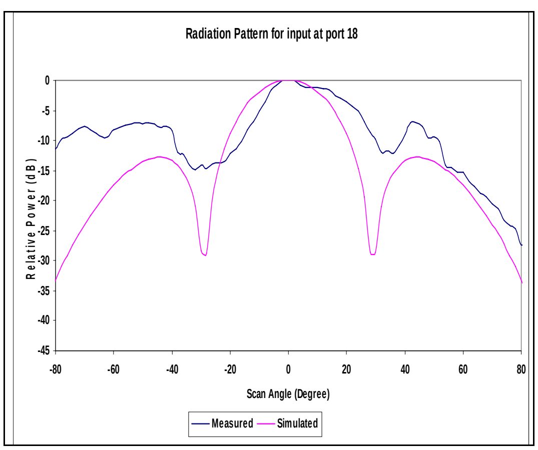

Fig. 11(a): Radiation pattern for input at port 18

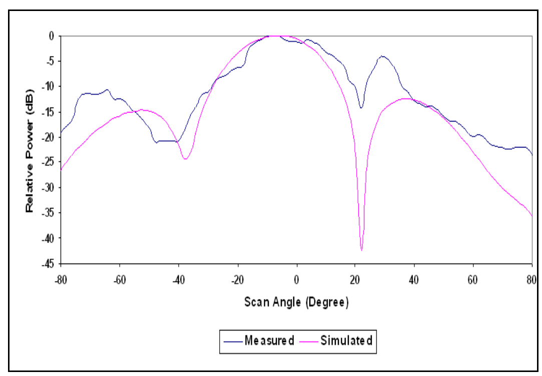

Fig. 11(b): Radiation pattern for input at port 19

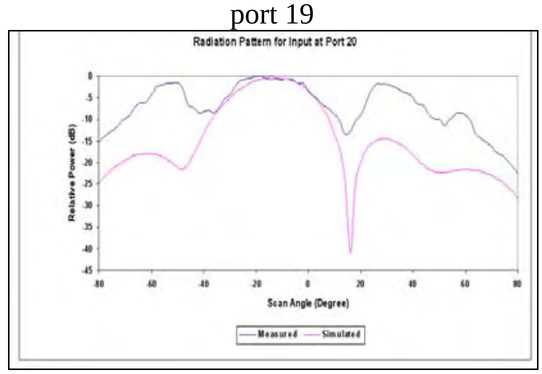

Fig. 11(c): Radiation pattern for input at port 20

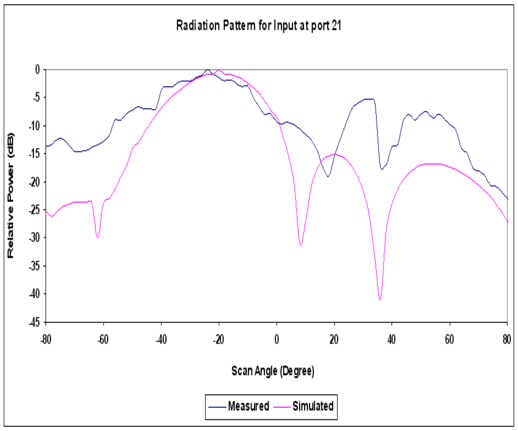

Fig. 11(d): Radiation pattern for input at port 21

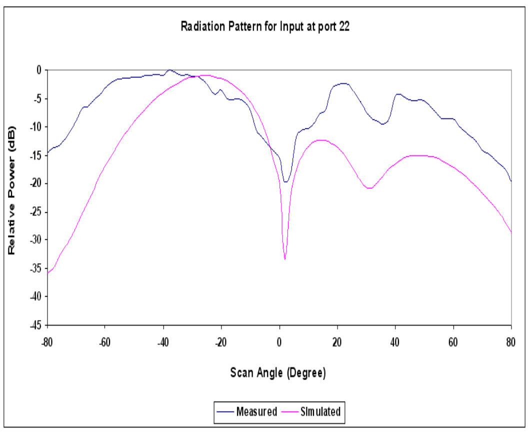

Fig. 11(e): Radiation pattern for input at port 22

Table 3, summarizes the radiation characteristics. The designed lens is covering an angular area from -38° to +38° and beam width from 24°to 28° has been obtained.

Table 3: Summary of the Radiation characteristics

Input	Direction of Outgoing Beam in Degree			3 dB Beam width in Degree	
	Measured	Simulated	Ideal	Measured	Simulated
18	0	0	0	24	24
19	-9	-8	-8.75	24	24
20	-19	-15	-17.5	25	25
21	-24	-21	-26.25	25	24
22	-38	-32	-35	28	24

To obtain a narrow outgoing beam an array of microstrip antenna array was developed as shown in figure 12.

Fig. 12: Designed microstrip antenna

Figure 13, shows the variation of return loss with frequency, the antenna is operating at 2.00 GHz.

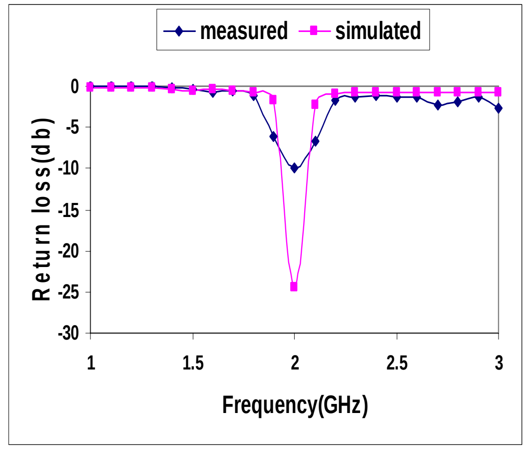

Fig. 13: Variation of Return loss with frequency

Figure 14 shows the photograph of the 10 units of radiating elements. The radiating elements were feed by the developed bootlace lens.

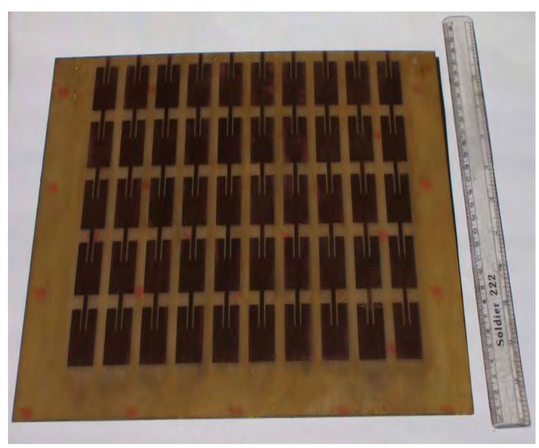

Fig. 14: Photograph of the developed microstrip antenna

Figure 15(a-d) shows the radiating pattern of the outgoing beam for input at different feed ports of the bootlace lens. A narrow beam has been obtained by using microstrip antenna in array; however there is no change in the direction of the outgoing beam.

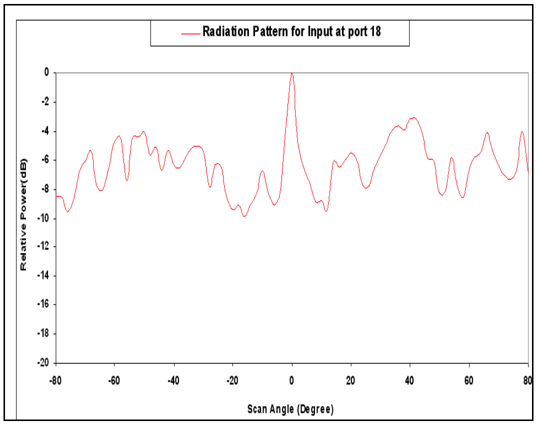

Fig. 15(a): Radiation pattern for input at port 18

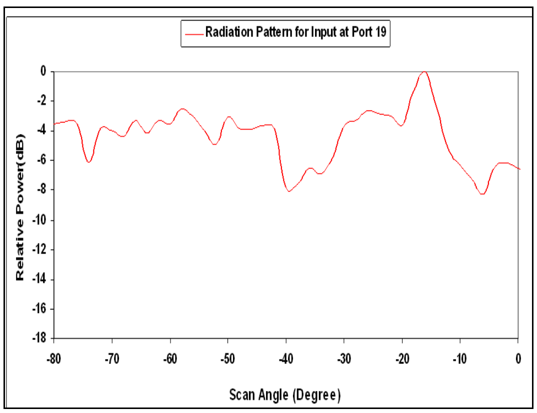

Fig. 15(b) : Radiation pattern for input at port 19

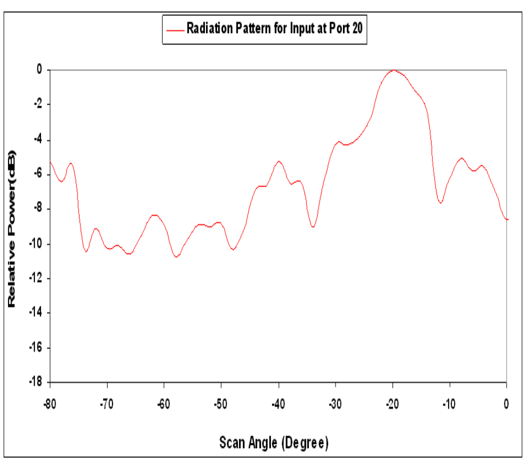

Fig. 15(c): Radiation pattern for input at port 20

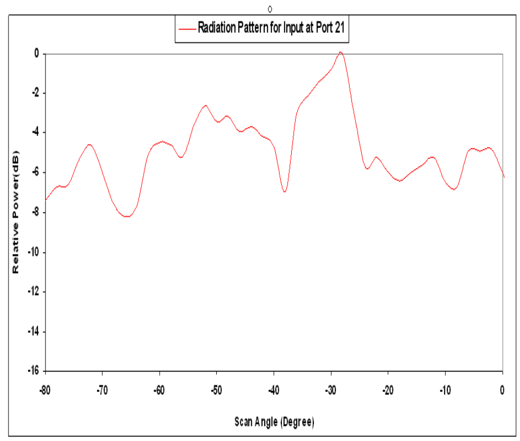

Fig. 15(d): Radiation pattern for input at port 21

III. CONCLUDING REMARKS

Microwave bootlace lens to fed antenna array at 2.0GHz has been developed on low cost material Glass Epoxy. Scattering matrix of the developed bootlace have been evaluated using the contour integral approach. Simulated results are in close agreement with the experimental results. Radiation characteristics of the lens have been determined with microstrip antenna and cascaded microstrip antenna. A narrow outgoing beam has also been obtained.

ACKNOWLEDGEMENT

Authors would like to acknowledge the financial support of Dept. of Science and Technology, Govt. of India.

REFERENCES

[1] W. Rotman and R.F. Turner, "Wide angle microwave lens for line source applications", IEEE Trans. on Antennas Propagat,, Vol. AP-11, pp23-632, Nov. 1963.

[2] G. Larry Leonakis, "Correction to wide angle microwave lens for line source applications", IEEE Trans Antennas Propagat. Vol. 36, p1067, Aug. 1986.

[3] J. Butler and Lowe R., "Beam forming matrix simplifies design of electronically scanned antennas", Electronics Design, 9, pp170-173, 1961.

[4] T. Katagi, S. Mano and Shin-Ichi Sato, “An improved design method of Rotman lens antennas”, IEEE Trans. On Antenna and Porpagation, Vol. AP-32, pp524-527, May 1984.

[5] D.R. Gagnon, “Procedure for correct refocussing of the Rotman Lens according to Snell’s Law”, IEEE Trans. On Antenna and Propagation, vol. 37, No. 3, pp390=392, March 1989.

[6] P.K.Singhal, P.C. Sharma and R.D. Gupta, “Rotman lens with equal height of array and feed contours”, IEEE Trans. On Antenna and Propagation, vol. 51, Issue 8, pp2048-2056, Aug. 2003.

[7] R.C. Hansen, “Design trades for Rotman Lens”, IEEE Trans. On Antenna and Propagation, Vol. 39, No. 4, pp464-472, April 1992.

[8] A.F. Peterson and E.O. Rausch, “Scattering matrix integral equation analysis of the design of a waveguide Rotman lens”, IEEE Trans. On Antenna and Propagation, Vol. 47, No. 5, pp 870-878, May 1999.

[9] N. Yuan, J.S. Kot and A.J. Parfitt, “Analysis of Rotman lenses using a hybrid least squares FEM/trsnafinite element method”, IEE proceedings Microwaves, Antennas and Propagation, Vol. 148, Issue 3, pp193-198,June 2001.

[10] E. Sbarra, L. Marcaccioli, R.V. Gatti and R. Sorrentino, “A novel Rotman lens in SIW technology”, European Microwave Conference, pp 1515-1518, Oct. 2007.

[11] Jaeheung kim, Choon Sik Cho and F.S. Barnes, “Dielectric slab Rotman lens for microwave/millimeter wave applications”, IEEE Trans. On Microwave Theory and Technique, Vol. 53, No.8, pp2622-2627, Aug. 2005.

[12] A. Sinjari and S. Chowdhury, “Design of a PZT based MEMS Rotman lens”, Canadian Conference on Electrical and Computer Engineering 2008, pp1121-1124, May 2008.

[13] H.H. Fuchs and D. Nussler, “Design of Rotman lens for beamsteering of 94GHz antenna array”, Electronics Letters, Vol. 35, No. 11, pp854-855, May 1999.

[14] T.K. Anthony, “Rotman lens development”, IEEE antenna and propagation society international symposium july 2008, pp1-4.

[15] T. Okoshi and T. Miyoshi, “The planar circuits – An approach to microwave integrated circuitry” IEEE Tans. On Microwave Theory and Tech., Vol. MTT-20, April 1972, pp245-252.

[16] T. Okoshi, “Planar circuits for microwave and light waves”, Springer Series Electrophys., Vol.18, 1984.

[17] R. Chadha and K.C. Gupta, “Segmentation method using impedance matrices for analysis of planar microwave circuits”, IEEE Trans. On Microwave Theory and Tech. , Vol. MTT-29, Jan. 1981, pp71-74.

[18] IE3D, Zeland Corp, U.S.A.